# Conformations and Solution Structure of Polyelectrolytes in Poor Solvent

*Hans Jörg Limbach, Christian Holm,* Kurt Kremer*

Max-Planck-Institut für Polymerforschung, Ackermannweg 10, 55128 Mainz, Germany; Fax: (+49) 6131 379100; Email: {limbach, holm, kremer}@mpip-mainz.mpg.de

**Summary:** Using extensive Molecular Dynamics (MD) simulations we study the behavior of polyelectrolytes in poor solvents, where we take explicitely care of the counterions. The resulting pearl-necklace structures are subject to strong conformational fluctuations, only leading to small signatures in the form factor, which is a severe obstacle for experimental observations. In addition we study how the necklace collapses as a function of Bjerrum length. At last we demonstrate that the position of the first peak in the inter-chain structure factor varies with the monomer density close to $\rho_m^{1/3}$ for all densities. This is in strong contrast to polyelectrolyte solutions in good solvent.

**Keywords:** polyelectrolytes, hydrogels, computer modeling, molecular dynamics, solution properties

## Introduction

Polyelectrolytes (PEs) are polymers which have the ability to dissociate charges in polar solvents resulting in charged polymer chains (macroion) and mobile counterions. They represent a broad and interesting class of soft matter [1, 2] that enjoy an increasing attention in the scientific community. In technical applications PEs are used as viscosity modifiers, as precipitating agents, and as superabsorbers. A thorough un-

 DOI: 10.1002/masy.200450703

derstanding of charged soft matter has become of great interest also in biochemistry and molecular biology. This is due to the fact that virtually all proteins, as well as other biopolymers such as DNA, actin, or microtubules are PEs.

Many PEs have a hydrocarbon based backbone for which water is a very poor solvent. Therefore, in aqueous solution, there is a competition between solvent quality, Coulombic interaction, and entropic degrees of freedom. The conformation of individual chains can under certain conditions assume pearl-necklace like structures[3, 4, 5]. In earlier simulations[6, 7] we found that the polymer density can be used as a very simple parameter to separate different conformational regimes. Here we analyze in more detail the single chain behavior and the scaling of the peak in the inter-chain structure function.

## Simulation Model

Our PE model and molecular dynamics (MD) approach has been described in Refs. [6, 7, 8, 9, 10] and consists of a bead spring chain of Lennard-Jones (LJ) particles. Chain monomers interact via a LJ interaction up to a distance $R_c = 2.5\sigma$ and experience an attraction with $\epsilon = 1.75\, k_B T$. The $\Theta$-point for this model is at $\epsilon = 0.34 k_B T$ [6]. The counterions interact via a purely repulsive LJ interaction. For bonded monomers we add a FENE bond potential. Charged particles at separation $r$ interact via the Coulomb energy $k_B T \ell_b q_i q_j / r$, with $q_i = 1, (-1)$ for the charged chain monomers (counterions) and the Bjerrum length $\ell_b = e^2/(4\pi\epsilon_S\epsilon_0 k_B T)$ ($e$: unit charge, $\epsilon_0$ and $\epsilon_S$: permittivity of the vacuum and of the solvent). We simulated various systems with several chains in the central simulation box at various monomer densities $\rho_m$ and different values of $\ell_b$. Each chain consists of $N_m = 48 \ldots 478$ monomers, with a

charge fraction $f = 1 \ldots 1/3$. The pressure $p$ was found to be always positive, with the $pV$ diagram being convex at all densities, thus our simulations are stable, reach true thermal equilibrium, and reside in a one phase region.

## Single Chain Properties

With the help of a specially developed cluster algorithm[8, 10] that automatically recognizes the number of pearls in a conformation, we have analyzed all equilibrium conformations in our systems. We found large coexistence regimes between structures consisting of conformations with different pearl numbers. Even a single chain shows over the course of time many transitions between different pearl structures, hence the different pearl states are not frozen or metastable. Also the position and size of the pearls and strings is constantly changing[8, 9], compare Fig.1. We furthermore found, that the lower the pearl number, the stronger the counterions are attracted to the pearls. This is easy to rationalize, since smaller number of pearls mean larger pearls due to mass conservation, and thus to a higher local charge density. The integrated ion distribution versus the chain distance displays an inflection point, which is a signal of counterion condensation[11]. In contrast to analytical theories[12], the pearl structures are stable, even though there are counterions localized near and/or inside the pearls.

When one starts in a necklace conformation and increases $\ell_b$ the counterions will get attracted more and more towards the chain. Scaling theories have predicted that with the onset of condensation the necklace state should collapse in a first order transition into the globular state[13, 5, 12, 14]. However, the 'onset' of condensation is not a sharp border, rather like within Poisson-Boltzmann theory one finds a smooth

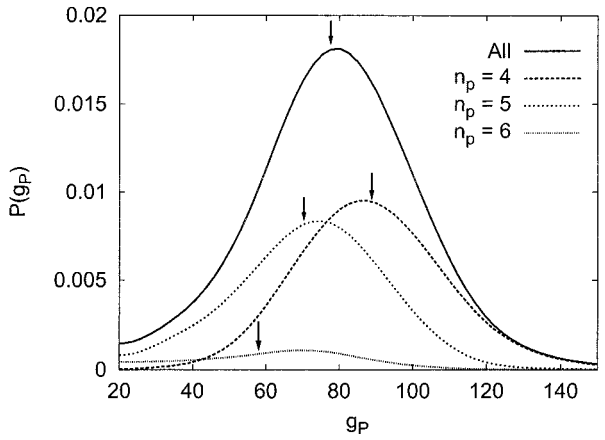


Figure 1: Probability distributions $P$ for the pearl size $g_P$ for a system with chain length $N_m = 382$, $\ell_b = 1.5\sigma$, and $f = 1/3$. Shown is the distribution for all chains as well as the distributions for the different structure types. The arrows mark the mean value of the corresponding probability distribution.

distribution of counterions which gets weighted closer to the macroion as the coupling is increased[11]. Accordingly, in the simulation we do not observe a collapse transition. The picture is qualitatively the same as in the good solvent case[15]. At $\ell_b = 0$ (no electrostatic interaction) the chain is in a collapsed conformation. By increasing $\ell_b$ the chain first extends up to a maximum, and then slowly shrinks back to a collapsed state. The non-monotonic behavior of the extension is qualitative the same as in the good solvent case[15] however the decrease is faster and more pronounced here[6, 16]. There is also a subtle dependence on $f$. The scaling variable which determines $R_E$ of the necklace is $f^2\ell_b$ at fixed $N_m$ and $\epsilon$[5]. In Fig.2 we show snapshots of chains with

the same value of $f^2\ell_b$, but different $f$. The chain extension is drastically different, and depends on the local interactions mediated by the counterions. This effect is obviously not captured by the scaling Ansatz! Note also, that the conformations on the way to the collapsed globule are very much reminiscent of a cylindrical shape[13], since the strings become very short, and the pearls coalesce slowly on a sausage like string until they reach the globular state. The collapsed state is reached roughly at the same value of $\ell_b$, which is reminiscent of the critical point of a Coulomb fluid.

Next we computed the spherically averaged form factor $S_1(q)$ of a single chain, shown in Fig.3, since this is an observable that is accessible in experiments, and for which also theoretical expressions have been developed[5, 17, 18].

In the range $1 < q\sigma < 2$ we denote a sharp decrease in $S_1$, which reflects the intra pearl scattering, because it shows the typical Porod scattering of $S_1(q) \simeq q^{-4}$. The kink at $q\sigma \approx 1.66$ appears at the position expected from the pearl size, but is broadly smeared out due to large size fluctuations. The shoulder which can be seen at $q\sigma \approx 0.5$ does not come from the intra-pearl scattering but is due to the scattering of neighboring pearls along the chain (inter-pearl contribution), which have a mean distance of $\langle r_{PP} \rangle = 13.3.\sigma$. It is also smeared out due to the large distribution of inter-pearl distances. We conclude that the signatures of the pearl-necklaces are weak already for monodisperse samples. A possible improvement could be achieved for chains of very large molecular weights and low pearl numbers, which could lead to stable and large signatures.

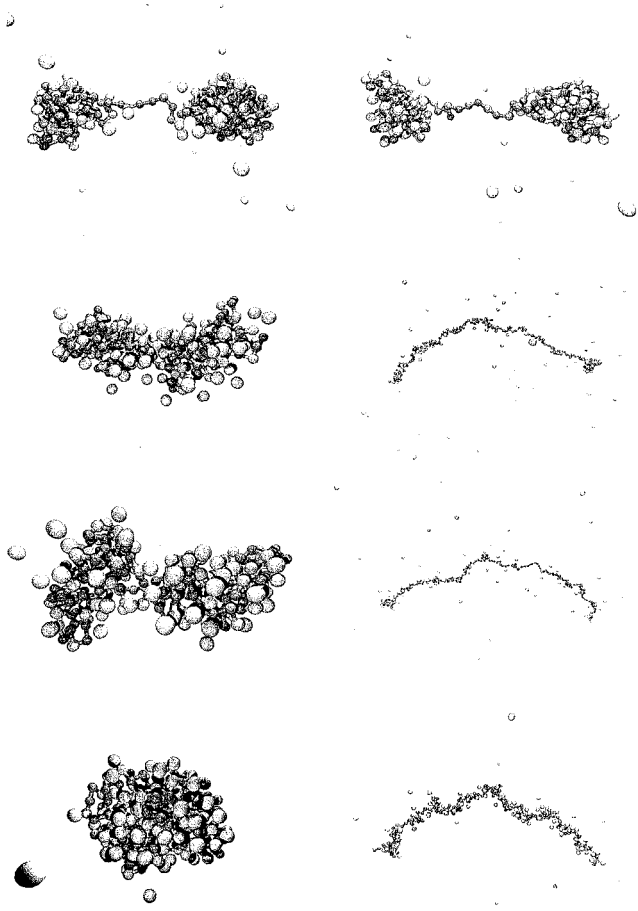

Figure 2: Snapshots for different values of the scaling variable $f^2\ell_b$. Left row with $f = 1/3$, right row with $f = 1/2$. From top to bottom $f^2\ell_b$ has the values: $0.08\sigma$, $0.25\sigma$, $0.5\sigma$, $1.0\sigma$. System: 8 chains with $N_m = 199$ monomers at $\rho_m = 5.0 \times 10^{-5}\sigma^{-3}$.

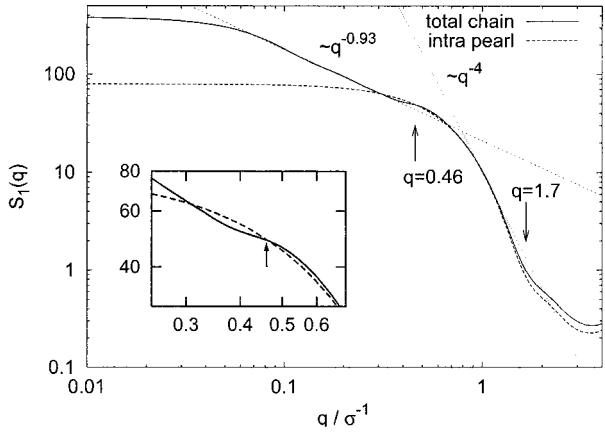


Figure 3: Spherically averaged form-factor $S_1(q)$. Shown are the single chain form-factor (solid line), together with the part of the form factor coming from the intra-pearl scattering (dashed line). The dotted and short dashed fits show the elongated chain part, and the Porod scattering part (globular conformation). System: 7 chains with 382 monomers, $f = 1/3$, $\ell_b = 1.5\sigma$, $\rho_m = 1.0 \times 10^{-5}\sigma^{-3}$.

## Scaling of the Correlation Length $\xi$ in Solution

The overall scattering function $S(q)$ of the solution contains additional experimental information. For good solvent PEs, experiments [19], theory [20], and simulations [15] find a pronounced first peak of $S_{IC} = S/S_1$ at $q^* = (2\pi)/\xi$, where $\xi$ is the correlation length. The position varies as $q^* \propto \rho_m^{1/3}$ in the very dilute regime and crosses over to a $\rho_m^{1/2}$ regime at higher concentrations. In Fig. 4 we have plotted the density dependence of $q^*$ in poor solvent for different chain lengths. Within the error bars we find that for poor solvent chains $q^*$ scales proportional to $\rho_m^{0.35\pm0.04}$ for *all* concentrations and

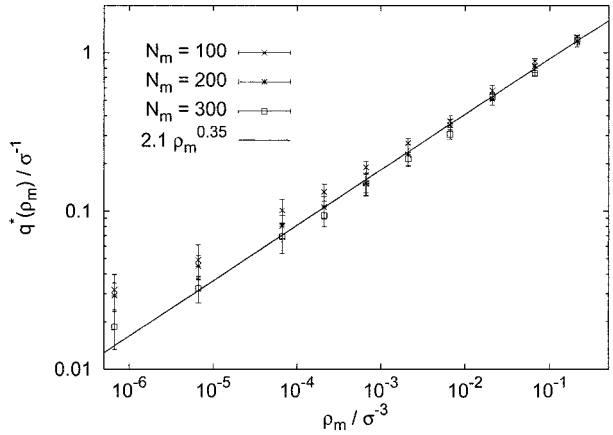


Figure 4: Density dependence of the peak $q^*$ in the structure factor for three different chain length $N_m = 100, 200, 300$ with $f = 0.5$ and $\ell_b = 1.5\sigma$. The black line is a fit to the data with $N_m = 200$.

chain lengths. This is in accord with very recent experiments[21], but theoretically not well understood. The response of the PE conformation to density changes is much larger in the poor solvent case [6, 8] than in the good solvent case [15], and the chain extension behaves non-monotonic as a function of density [6, 8]. Furthermore, in the density regime between $\rho_m\sigma^3 = 10^{-2} \ldots 10^{-4}$ the chain extension and the pearl number varies most strongly, and almost all monomers are located within the pearls. Upon approaching the dense regime, the string length tends to zero and we find a chain of touching pearls, indicating that the conventional necklace picture breaks down. Our result is compatible to scaling exponents found in scattering experiments [17, 22, 23].

Scaling theories[24, 25] have predicted a $\rho_m^{1/2}$ regime to start at $\rho_o^*$, which is defined

at the density where $R_E \approx \xi$, and to extend until $\xi \approx r_{pp}$ where a bead-controlled $\rho_m^{1/3}$ regime starts. We find $\rho_o^* \sigma^3 \simeq 5 \times 10^{-2}, 10^{-3}, 10^{-4}$ for $N_m = 100, 200, 300$. A pearl-pearl separation of the order of the correlation length length, $r_{pp} \approx \xi$, is reached between $\rho_m \sigma^3 = 10^{-2}$ and $10^{-1}$, which is roughly independent of $N$. Especially for the longer chains ($N_m = 200, 300$) a clear signature of a different power law, i.e.$\rho_m^{1/2}$, should be visible. One possible reason for our different findings is that the strong inter-chain coupling and the influence of the counterions on the conformations are not sufficiently taken into account in the (mean field) scaling approach. It is not clear at this stage if the $\rho_m^{1/2}$ regime can be recovered for much longer chain length. In addition we observe that the chains form a transient physical network at $\rho_m \sigma^3 = 0.2$ for $N_m \geq 200$ which has neither been seen in previous simulations nor predicted by theoretical approaches but is in accord with experimental studies [17, 22, 23]. During the simulation time these networks reconstruct several times, e.g. chains are not trapped!

A more detailed account of the presented material will be published in forthcoming publications[10, 26].

## Acknowledgments

We gratefully acknowledge partial funding through the "Zentrum für Multifunktionelle Werkstoffe und Miniaturisierte Funktionseinheiten", grant BMBF 03N 6500, and the DFG through the SFB 625 and the TR 6.

[1] *Polyelectrolytes: Science and Technology*, M. Hara Ed., Marcel Dekker, New York, 1993.

[2] *Electrostatic Effects in Soft Matter and Biophysics*, Vol. 46 of *NATO Science Series II - Mathematics, Physics and Chemistry*, C. Holm, P. Kékicheff, and R. Podgornik, Eds. Kluwer Academic Publishers, Dordrecht, NL, 2001.

[3] Y. Kantor, M. Kardar, Europhys. Lett. **1994**, *27*, 643 .

[4] Y. Kantor, M. Kardar, Phys. Rev. E **1995**, *51*, 1299.

[5] A. V. Dobrynin, M. Rubinstein, S. P. Obukhov, Macromolecules **1996**, *29*, 2974.

[6] U. Micka, C. Holm, K. Kremer, Langmuir **1999**, *15*, 4033.

[7] H. J. Limbach, C. Holm, J. Chem. Phys. **2001**, *114*, 9674.

[8] H. J. Limbach, Ph.D. thesis, Johannes Gutenberg Universität, Mainz, Germany, 2001, available at http://archimed.uni-mainz.de/pub/2002/0121/

[9] H. J. Limbach C. Holm, Comp. Phys. Comp. **2002** *147*, 321; H. J. Limbach, C. Holm, K. Kremer, Europhys. Lett. **2002** *60*, 566.

[10] H. J. Limbach C. Holm, J. Phys. Chem B **2003**, *107*, 8041.

[11] M. Deserno, C. Holm, S. May, Macromolecules **2000**, *33*, 199.

[12] H. Schiessel P. Pincus, Macromolecules **1998**, *31*, 7953.

[13] A. Khokhlov, J. Phys. A **1980**, *13*, 979.

[14] T. A. Vilgis, A. Johner, J.-F. Joanny, Eur. Phys. J. E **2000**, *2*, 289.

[15] M. J. Stevens, K. Kremer, J. Chem. Phys. **1995**, *103*, 1669.

[16] M. Khan, S. Mel'nikov, B. Jönsson, Macromol. **1999**, *32*, 8836.

[17] C. Heitz, M. Rawiso, J. François, Polymer **1999**, *40*, 1637.

[18] R. Schweins, K. Huber, preprint; see also contribution in this volume.

[19] M. Nierlich *et al.*, J. Physique **1979**, *40*, 701.

[20] J. F. Joanny, in *Electrostatic Effects in Soft Matter and Biophysics*, Vol. 46 of *NATO Science Series II - Mathematics, Physics and Chemistry*, C. Holm, P. Kékicheff, and R. Podgornik. Eds., Kluwer Academic Publishers, Dordrecht, NL, 2001, pp. 149–170.

[21] D. Baigl , R. Ober, D. Quo, A. Fery, C. E. Williams, Europhys. Lett. **2003**, *62*, 588.

[22] W. Essafi, F. Lafuma, C. E. Williams, J. Phys. II **1995**, *5*, 1269.

[23] T. A. Waigh, R. Ober, C. E. Williams, J.-C. Galin, Macromolecules **2001**, *34*, 1973.

[24] A. V. Dobrynin, M. Rubinstein, Macromolecules **1999**, *32*, 915.

[25] A. V. Dobrynin, M. Rubinstein, Macromolecules **2001**, *34*, 1964.

[26] H. J. Limbach, C. Holm, K. Kremer, in preparation.